

# Sandwiched liquid metal membrane (SLiMM) for hydrogen purification

*Pei-Shan Yen, Nicholas D. Deveau and Ravindra Datta\**

## Significance

Palladium-based membranes are currently the most advanced membranes for hydrogen separation and are on the verge of practical application. However, the search for alternative membranes continues in an effort to lower their cost and susceptibility to poisons. Here for the first time we report a novel sandwiched liquid metal membrane (SLiMM) for hydrogen separation. Permeation experiments indicate that the Ga/SiC SLiMM has a permeability of  $2.75 \times 10^{-7}$  mol/ms·Pa<sup>0.5</sup> at 500 °C, which is 35 time higher than Pd under similar conditions.

Hydrogen has been touted as an energy carrier in the so-called “hydrogen economy,”<sup>1</sup> which envisions its widespread generation, distribution, and storage. Hydrogen is industrially produced from natural gas via steam reforming at 25 atm. and 800 – 950 °C followed by water gas shift reaction to produce a reformat gas (H<sub>2</sub> + CO<sub>2</sub>),<sup>2</sup> from which H<sub>2</sub> is separated and purified typically via the energy-intensive pressure swing adsorption process. Thin (~ 20 μm) but dense palladium membranes, coated on porous metal or ceramic supports, are being developed as an alternate and more efficient process to produce high purity H<sub>2</sub>,<sup>2,3</sup> along with concentrated CO<sub>2</sub> suitable for sequestration. However, Pd is too expensive, sensitive to poisons, and has limited stability at the temperatures employed (500 °C or higher).<sup>4,5</sup> Consequently, cheaper and more abundant metals have also been investigated as H<sub>2</sub> membranes (Figure 1). In fact, many

---

P. S. Yen, N. D. Deveau, Prof. R. Datta  
Fuel Cell Center, Department of Chemical Engineering  
Worcester Polytechnic Institute  
Worcester, Massachusetts 01609, USA.  
E-mail: rdatta@wpi.edu

This is the author manuscript accepted for publication and has undergone full peer review but has not been through the copyediting, typesetting, pagination and proofreading process, which may lead to differences between this version and the [Version record](#). Please cite this article as [doi: 10.1002/aic.15658](https://doi.org/10.1002/aic.15658).

This article is protected by copyright. All rights reserved.

amorphous metals have attractive hydrogen permeability, as shown in Figure 1, but they tend to become crystallized at the higher operating temperatures leading to permeability decay, and further often require a Pd surface coating to facilitate dissociative surface H<sub>2</sub> adsorption, the first step in hydrogen permeation.<sup>6-9</sup> The advantage of using liquid metal membrane can overcome many of the issues with solid metal membrane such as sintering, hydrogen embrittlement, and thermal mismatch between the membrane and the support.

Only dense solid metals have so far been considered as H<sub>2</sub> membranes. Here, for the first time we demonstrate the feasibility of a sandwiched liquid metal membrane (SLiMM) for H<sub>2</sub> purification, using gallium as an example. Although there are numerous other possible liquid metal/alloy candidates, gallium was picked for these initial studies because of its low melting point (29.8 °C), low cost, relative abundance, low toxicity, and very low vapor pressure making significant evaporation losses unlikely even over extended time at 500 °C.

Measured hydrogen permeability of liquid Ga at 500 °C (Figure 1) is roughly 35 times higher than that of Pd,<sup>6</sup> while its price is an order of magnitude lower.<sup>10</sup> Development of such high performing and inexpensive membranes could bring the H<sub>2</sub> economy a step closer to reality.

The proposed SLiMM comprises a thin (~ 200 μm) film of a liquid metal or alloy, sandwiched between two inert porous ceramic supports (Figure 2). This is an order of magnitude thicker than state-of-the-art Pd membranes, but provides good flux due to its higher permeability while ensuring robustness and denseness.

The mechanism of hydrogen permeation through a solid metal, especially Pd membrane, is well investigated.<sup>6</sup> A similar mechanism is known to be operative in a liquid metal. Thus, the solution and diffusion of H<sub>2</sub> and its isotopes in some liquid metals and alloys has been investigated in connection with their use as liquid breeder and coolant materials in nuclear fusion reactor.<sup>11</sup> As

depicted in Figure 2, hydrogen permeation in SLiMM involves the following sequential steps:<sup>12</sup>

① the H<sub>2</sub> molecules on the feed side dissociatively adsorb on the metal surface as H atoms, ② which next infiltrate the bulk lattice as interstitial H atoms, ③ then diffuse across the membrane, and ④ upon reaching the permeate side egress from the bulk metal to its surface, and finally ⑤ the adsorbed H atoms on permeate-side metal surface recombine and desorb as H<sub>2</sub> molecules.

The solubility of hydrogen in liquid metals in the limit of dilute solutions is known to be described by Sieverts' law,<sup>13</sup> much as it is in solid metals, i.e.,

$$x_{\text{H-M}} \approx K_S \sqrt{p_{\text{H}_2} / p^\circ} \quad ; \quad K_S = \exp\left(\frac{\Delta S_S^\circ}{R} - \frac{\Delta H_S^\circ}{RT}\right) \quad (1)$$

where  $x_{\text{H-M}}$  is the H/M mole fraction of interstitial H in the metal,  $K_S$  is the so-called Sieverts' equilibrium constant, given in terms of  $\Delta S_S^\circ$  and  $\Delta H_S^\circ$ , the standard entropy and enthalpy change of hydrogen solution in the metal, respectively. Further,  $R$  is the gas constant,  $T$  is the temperature,  $p_{\text{H}_2}$  is the hydrogen partial pressure, and  $p^\circ$  is the standard pressure (1 atm.). For hydrogen solution in Pd, for instance,  $\Delta H_S^\circ = -12.1$  kJ/mol, and  $\Delta S_S^\circ = -63$  J/mol K.<sup>12</sup>

At lower temperatures (350 °C or less), H<sub>2</sub> permeation flux  $N_{\text{H}_2}$  is typically limited by surface adsorption/desorption rates, namely, steps ① and ⑤.<sup>12</sup> At higher temperatures that are more typical of practical application, however, the diffusion of the interstitial H atoms within the bulk metal is the rate-determining step (RDS). Then, combining Fick's law for interstitial H atom diffusion with Sieverts' law for H solution provides the H<sub>2</sub> flux through the metal membrane

$$N_{\text{H}_2} \approx P_{\text{H}_2} \left( p_{\text{H}_2, f}^{1/2} - p_{\text{H}_2, p}^{1/2} \right) \quad (2)$$

where the hydrogen *permeance* of the membrane

$$P_{\text{H}_2} \equiv \left( \frac{1}{2V_M \sqrt{p^\circ}} \right) \frac{K_S D_{\text{H}}}{\delta} \quad (3)$$

Here  $D_H$  is the interstitial diffusion coefficient of H atoms,  $V_M$  is the molar volume of metal M (e.g.,  $V_M = 8.85 \text{ cm}^3$  per g atom Pd), and  $\delta$  is the dense metal membrane thickness. The factor 2 in the denominator accounts for interstitial diffusion of two H atoms per  $\text{H}_2$  molecule. An alternate transport characteristic commonly used is membrane *permeability*, i.e.,

$$Q_{\text{H}_2} = P_{\text{H}_2} \delta \quad (4)$$

which has the virtue of involving only material properties, not membrane thickness.

These two related permeation parameters,  $P_{\text{H}_2}$  and  $Q_{\text{H}_2}$ , have an Arrhenius temperature dependence<sup>12</sup> with an effective activation energy  $E$ , just as does the atomic H diffusion coefficient with an effective activation energy  $E_D$

$$D_H = D_{H,0} \exp\left(-\frac{E_D}{RT}\right) \quad (5)$$

where  $D_{H,0}$  is the pre-exponential factor. The effective activation energy for  $P_{\text{H}_2}$  and  $Q_{\text{H}_2}$ , thus,  $E = E_D + \Delta H_S^\circ$ . For Pd, for instance,  $E_D = 27 \text{ kJ/mol}$ , so that  $E = 27 + (-12.1) = 14.9 \text{ kJ/mol}$ .<sup>12</sup> Thin Pd membranes ( $\delta \sim 20 \text{ }\mu\text{m}$ ) are now used to increase  $\text{H}_2$  permeance and reduce costs. A further reduction in thickness is needed, however, to make Pd membranes cost-effective, which makes them less rugged. Thicker membranes, on the other hand, while being more robust and resistant to cracking or pin-hole formation, have a lower permeance (Eq. 3), and thus require a larger membrane area  $A_M$  for a given hydrogen production rate,  $\dot{n}_{\text{H}_2} = N_{\text{H}_2} A_M$ . As an example, if membrane thickness  $\delta$  is doubled, so must the area  $A_M$ , thus quadrupling the amount ( $\delta \times A_M$ ) and the cost of Pd that is needed. On the other hand, if we could double the permeability  $Q_{\text{H}_2}$ , the thickness could be doubled to provide a more robust membrane without increasing its area, as accomplished here with SLiMM.

In fact, we can expect substantially higher hydrogen permeance in liquid metals than in solid metals, exclusively investigated so far as H<sub>2</sub> membranes, as the available evidence suggests that hydrogen solubility as well as diffusivity in liquid metals is higher. Thus, as shown in Figure 3 for some common metals,<sup>12,14-17</sup> hydrogen solubility in their liquid state is higher than in their solid state. In fact, a step increase in solubility is typically observed at the melting point, as shown in Figure 3 for the examples of Mg, Al, Cu, and Ni. This is evidently a result of the increased interstitial space in the bulk metal upon melting.

Since there are no reports so far of H<sub>2</sub> solubility in liquid gallium, we used the Sieverts' apparatus,<sup>16,18,19</sup> to experimentally investigate hydrogen uptake in liquid Ga by employing hydrogen at various pressures and temperatures (350 – 500 °C) over a pool of Ga contained in a graphite crucible. The chamber was first evacuated thoroughly and then 1 atm. of hydrogen was introduced. The subsequent pressure change over time because of absorption was recorded via a data acquisition system, and used to calculate the amount of hydrogen absorbed by the liquid gallium.

The measured solubility for hydrogen in liquid gallium versus inverse temperature is shown in Figure 3. The calculated heat of solution from the data in Figure 3 provides  $\Delta H_s^\circ = +15.76$  kJ/mol while the entropy change is  $-5.45$  J/mol K. Thus, hydrogen solubility in liquid Ga in Figure 3 is seen to be higher than that of Pd in the temperature range of interest (350 – 500 °C).

Furthermore, even though the diffusion coefficient of H atoms in solid metals is much higher than that of the other atomic impurities such as C or O, which accounts for the extraordinarily high selectivity of Pd membranes for hydrogen permeation, it is typically higher by an order of magnitude in liquid metals. Thus, Figure 4 provides examples of H diffusion coefficient in some metals in their liquid and solid states as a function of inverse absolute temperature.

It further shows a step increase in H diffusivity of a metal upon melting, also presumably due to the increased interstitial space. The H diffusion coefficient in liquid Ga is reported in the literature,<sup>15</sup> namely,  $D_{H,0} = 0.003 \text{ cm}^2/\text{s}$  and  $E_D = 9.61 \text{ kJ/mol}$ , and is seen (Figure 4) to be an order of magnitude higher than that in Pd in the temperature range of interest.<sup>20</sup>

It is, thus, clear from Figures 3 and 4 that *both* the solubility  $x_{H,M}$  and the interstitial H atom diffusion coefficient  $D_H$  can be substantially higher, so that we may expect a substantially higher permeance, in a liquid metal as compared to a solid metal. This is the central hypothesis behind our proposal for using sandwiched dense liquid metal films as hydrogen membranes.

To confirm this thesis, we also measured the permeability of a supported liquid gallium membrane at various temperatures. To experimentally determine the hydrogen permeance of a liquid Ga membrane at various temperatures and pressures, a liquid Ga film was deposited on top of a porous substrate. Electroless and electro-plating are the most common techniques used for depositing thin Pd films typically on a porous metal substrate with an interfacial diffusion barrier layer to prevent inter-diffusion of Pd and the support metal at higher temperatures.<sup>23</sup> Unlike for Pd,<sup>6, 23</sup> however, porous metal substrates were found to be unsuitable for supporting liquid metal films, as the liquid metals readily react with most metallic substrates at the elevated temperatures ( $\sim 500 \text{ }^\circ\text{C}$ ) forming intermetallic compounds. Even many ceramic supports were found to be unsuitable as they reacted with the liquid metals at the higher temperatures, while others are overly inert and not adequately wetted by the liquid metal to form a thin liquid film. Just the right affinity (Gibbs free energy change) is needed between the liquid metal and the porous support to strike a balance between wettability and reactivity to form a free-standing and thin liquid metal film on top of an inert support.

To screen porous ceramic supports systematically for their suitability, thus, a thermodynamic analysis was performed for any potential reaction between liquid gallium and support ceramic (oxides, carbides, and nitrides) components at 500 °C. Thus, we found that many of the oxide ceramics supports such as SiO<sub>2</sub> and NiO were overly reactive, while others such as Al<sub>2</sub>O<sub>3</sub> and ZrO<sub>2</sub> were found to be stable, as were many carbides. Experiments were then performed to confirm these theoretical predictions, and in this manner we were able to select suitable porous ceramic supports for SLiMM that are both stable and adequately wettable, including the SiC and graphite supports used for the results reported here. Carbon based materials are very inert to liquid gallium, as they are unlikely to form GaC<sub>2</sub>,<sup>24</sup> making such membranes stable over time at high temperature.

To make the sandwich liquid membrane structure, the first step was to attach the porous SiC support disc at one end of a nonporous SiC tube. Thus, the 0.1 μm grade porous SiC disc (supplied by LiqTech) and the dense SiC tube (supplied by Saint Gobain) were cleansed via IPA prior sealing. Glass paste was applied to the interface between the tube and the disc multiple times in order to build a lip to contain liquid gallium pool and also to make sure that any gaps between the tube and the disc were completely sealed. After air drying for 30 minutes, the tube was then subjected to heat treatment. Glass paste 613 from Aremco, Inc., was selected on the basis of a compatible coefficient of thermal expansion, curing temperature, and material composition. The hence attached and sealed porous SiC disc and the nonporous SiC tube are shown in Figure 5 (a). Next, a weighed amount of gallium was placed on the porous substrate SiC and melted by heating lamp. When fully melted, a vacuum was applied on the SiC tube side to help spread and deposit the liquid gallium film as shown in Figure 5 (b). The deposited liquid

gallium was then put in a freezer to solidify the formed membrane. In its solid state, the gallium membrane is easier to transport and mount in the permeation cell assembly.

The other concern, however, that needed to be addressed for membrane stability is that the liquid metal surface tension and wettability is a function of temperature, pressure, as well as the gas composition.<sup>25</sup> Thus, it was found that when switching from hydrogen to helium during extended experiments to check for any leaks that might have developed, the membrane wetting could reduce due to an increase in the surface tension. A solution found to this issue was to select a sandwich configuration for SLiMM, with the liquid metal film supported between *two* porous substrates as shown schematically in Figure 1, thus obviating a free liquid metal surface exposed to the gas. For this, a sheet of graphene with a diameter slightly larger than that of the gallium was used to cover it. Glass paste was then applied to the interface between the graphene sheet and the glass sealant carefully. Upon heating to the permeation temperature, this graphene layer became affixed thus sandwiching the gallium layer as indicated in Figure 5 (c). This step was taken to avoid any free liquid gallium surface morphology change brought by surface tension and wettability change under a helium atmosphere. It may be mentioned that while the sandwiched configuration employed in these experiments was rigid, a compressible assembly will further allow fabrication of stable membranes.

The sandwiched liquid Ga membranes (274  $\mu\text{m}$  thick) thus fabricated was next tested for permeance and stability. The relatively large thickness of the membrane employed in this study was to ensure that the liquid film was dense and the hydrogen selectivity remained high in order to accurately characterize the membrane permeability. Membranes below 200  $\mu\text{m}$  were sometimes found to be leaky due to substrate wettability issue that needs to be resolved further. With proper substrate material and sandwich fabrication, the thickness of the membrane could be

reduced further. In fact, if some compression could be applied in the sandwiched configuration, wettability would be less of an issue and thinner dense membranes could be developed.

In this experiment, the liquid Ga membrane was tested at various temperatures between 480 – 550 °C, under 3 – 5 psig hydrogen atmosphere, continually over a period of two weeks to determine both the permeability at different temperatures and to confirm membrane stability.

The scheme of hydrogen permeation cell setup is shown in Figure 5 (d).

The membrane was found to be dense and the hydrogen permeation typically remained stable for roughly seven days. Thus, no helium was detected throughout this period during periodic switching from hydrogen to helium. The measured hydrogen permeability of dense membrane at 500 °C was found to be about 35 times higher than that of a Pd foil.<sup>6</sup> The temperature was varied between to obtain an activation energy of permeability,  $E = 49.5$  kJ/mol.

A sudden increase in permeance if observed would indicate development of a small leak, either as a pinhole in the glass seal or in the liquid membrane, and confirmed via detection of small amounts of He in the permeate, but often still with high hydrogen/helium selectivity,  $\alpha \equiv N_{\text{H}_2} / N_{\text{He}}$  in the range of 100 or above. The test would be terminated when H<sub>2</sub>/He selectivity dropped to  $\alpha = 25$ . Even this value is still substantially higher than that for Knudsen diffusion, i.e.,  $\alpha = 1.44$ ,<sup>26</sup> which would be obtained if the flux were entirely through pinholes, clearly indicating substantial flux through the metal despite the leak. The completely dense membrane typically for the first week, however, afforded an essentially infinite selectivity.

The hydrogen flux through Ga SLiMM was further compared with that calculated via Eq. (2) based on Sieverts' law with independently determined solubility and diffusivity, and the results are shown in Figure 6. The Sieverts' law constant used in Eq. (3) was measured from Sieverts' experiment as described above, while the diffusivity was taken as reported in the literature<sup>15</sup>.

Measured hydrogen flux is about 20 % lower than that calculated via Sievert's law from hence determined solubility and diffusivity. A possible reason for the deviation is that the hydrogen flux in a sandwiched structure may also be partly reduced by the resistance of the porous layers above and below the liquid layer. Another possible reason is that the independently measured hydrogen flux, solubility, and diffusivity all contain experimental error. Thus, if we assume a 10 % standard error in the independent hydrogen flux measurements, in solubility experiments, as well as in the reported diffusivity, the predicted results in Figure 6 seem to fall within the range of experimental error.

Based on the results presented here, thus, we can conclude that our hypothesis that liquid metal membranes should have high H<sub>2</sub> permeability because of high solubility and high diffusion coefficient at elevated temperatures has been shown to be correct. Both hydrogen diffusivity as well as solubility in liquid gallium was found to be higher than in Pd. This portends the development of non-Pd hydrogen membranes, which has long been elusive.<sup>7</sup> Measured permeability at 500 °C  $2.75 \times 10^{-7}$  mol/ms·Pa<sup>0.5</sup> is only lower than Nb and higher than all the amorphous alloys described in several articles<sup>6-9</sup> as summarized in Figure 1. This provides clear evidence that supported liquid gallium has a strong potential as a hydrogen separation membrane, although, considerable further study is needed before application, including with realist gas mixtures.

There are numerous other liquid metals and alloys that might be suitable for SLiMM and need to be tested. Further, any reaction with sulfur contamination present in syngas with liquid gallium membrane would need more investigation, though, there is no evidence of GaS formation below ~2 at% S (0.9 wt%) at 500 °C from Ga-S phase diagram,<sup>27</sup> thus offering the potential of good sulfur tolerance, which is the Achilles heel for Pd. Other, technological issues

such as suitable supports, sealing, and good membrane stability also remain to be fully resolved. Nonetheless, the scientific premise appears sound, and the potential practical application of SLiMM shows promise.

### Acknowledgment

We acknowledge financial support from the Department of Energy under award number DE-FE0001050. We are also thankful to Y. H. Ma, I. Fishtik, and I. Mardilovich for their help with membrane fabrication and discussions. We are grateful to R. Kapoor and A. Bakshi of Saint Gobain, Inc., Worcester, MA, for supplying the nonporous SiC tubes, and to J. Morgan of AvCarb Materials Solutions, Lowell, MA, for supplying graphene sheets.

### Literature Cited

1. Marbán G, Valdés-Solís T. Towards the hydrogen economy? *Int. J. Hydrogen Energy*. 2007;32:1625-1637.
2. Rostrup-Nielsen JR, Rostrup-Nielsen T. Large-scale hydrogen production. *Cattech*. 2002;6:150-159.
3. Armor JN. Applications of catalytic inorganic membrane reactors to refinery products. *J. Membr. Sci.* 1998;147:217-233.
4. Adams BD, Chen A. The role of palladium in a hydrogen economy. *Mater. Today*. 2011;14:282-289.
5. Ockwig NW, Nenoff TM. Membranes for hydrogen separation. *Chem. Rev.* 2007;107:4078-4110.
6. Ayturk ME, Kazantzis N, Ma YH. Modeling and performance assessment of Pd and Pd/Au-based catalytic membrane reactors for hydrogen production. *Energy Environ Sci.* 2009;2:430-438.

- . Phair JW, Donelson R. Developments and design of novel (non-palladium-based) metal membranes for hydrogen separation. *Ind. Eng. Chem. Res.* 2006;45:5657-5674.
- . Li X, Liu D, Liang X, Chen R, Rettenmayr M, Su Y, Guo J, Fu H. Substantial enhancement of hydrogen permeability and embrittlement resistance of Nb<sub>30</sub>Ti<sub>25</sub>Hf<sub>10</sub>Co<sub>35</sub> eutectic alloy membranes by directional solidification. *J. Membr. Sci.*, 2015;496:165-173.
- . Dolan M, Dave N, Morpeth L, Donelson R, Liang D, Kellam M, Song S. *J. Membr. Sci.* 2009;326:549-555.
0. USGS mineral commodity summaries 2015. *U. S. Dept.of the Interior, U. S. Geological Survey*, Reston, 2015.
1. Schumacher R, Weiss A. Ni-based amorphous alloy membranes for hydrogen separation at 400 °C. *Ber. Bunsenges.Phys.Chem.* 1990;94:684-691.
2. Deveau ND, Ma YH, Datta R. Beyond Sieverts' law: a comprehensive microkinetic model of hydrogen permeation in dense metal membranes. *J. Membr. Sci.* 2013;437:298-311.
3. Sieverts A. Absorption of gases by metals. *Z. Metallk.* 1929;21:37-46.
4. Hubberstey P. Hydrogen in liquid alkali metals. *J. Less Common Met.* 1976;49:253-269.
5. Fruehan RJ, Anyalebechi PN. Gases in metals. *ASM Handbook.* 2008;15:64-73.
6. Sacris EM, Parlee NAD. The diffusion of hydrogen in liquid Ni, Cu, Ag, and Sn. *Metall. Mater. Trans. B.* 1970;1:3377-3382.
7. Gale WF, Totemeier TC. Gas-metal systems. In: Gale WF, Totemeier TC. *Smithells metals reference book.* Oxford: Elsevier Butterworth-Heinemann, 2003: 12-1-12-28.
8. Blach TP, Gray EMA. Sieverts apparatus and methodology for accurate determination of hydrogen uptake by light-atom hosts. *J. Alloy Compd.* 2007;446-447:692-697.

9. Solar MY, Guthrie RIL. Hydrogen transport in stagnant molten iron. *Metall. Trans. A* 1971;2:457-464.
0. Mazayev SN, Prokofiev YG. Hydrogen inventory in gallium. *J. Nucl. Mater.* 1994;212-215:1497-1498.
1. Fisher DJ. Hydrogen diffusion in metals: a 30-year retrospective. Switzerland: Scitec Publications Ltd., 1999.
2. Toda G. Rate of permeation and diffusion coefficient of hydrogen through palladium. *J. Res. Inst. Catal. Hokkaido Univ.* 1958;6:13-19.
3. Ma YH, Akis BC, Ayturk ME, Guazzone F, Engwall EE, Mardilovich IP. Characterization of intermetallic diffusion barrier and alloy formation for Pd/Cu and Pd/Ag porous stainless steel composite membranes. *Ind. Eng. Chem. Res.* 2004;43:2936-2945.
4. Samsonov GV, Panasyuk AD, Kozina GK. Wetting of refractory carbides with liquid metals. *Powder Metall. Met. Ceram.* 1968;7:874-878.
5. Yen PS, Datta R. Butler-Sugimoto monomolecular bilayer interface model: the effect of oxygen on the surface tension of a liquid metal and its wetting of a ceramic. *J. Colloid Interface Sci.* 2014;426:314-323.
6. Datta R, Dechapanichkul S, Kim JS, Fang LY, Uehara H. A generalized model for the transport of gases in porous, non-porous, and leaky membranes I. Application to single gases. *J. Membr. Sci.* 1992;75:245-263.
7. Lieth RM, Heijligers HJ, vd Heijden CW. The P-T-X phase diagram of the system Ga-S. *J. Electrochem. Soc.* 1966;113:798-801.

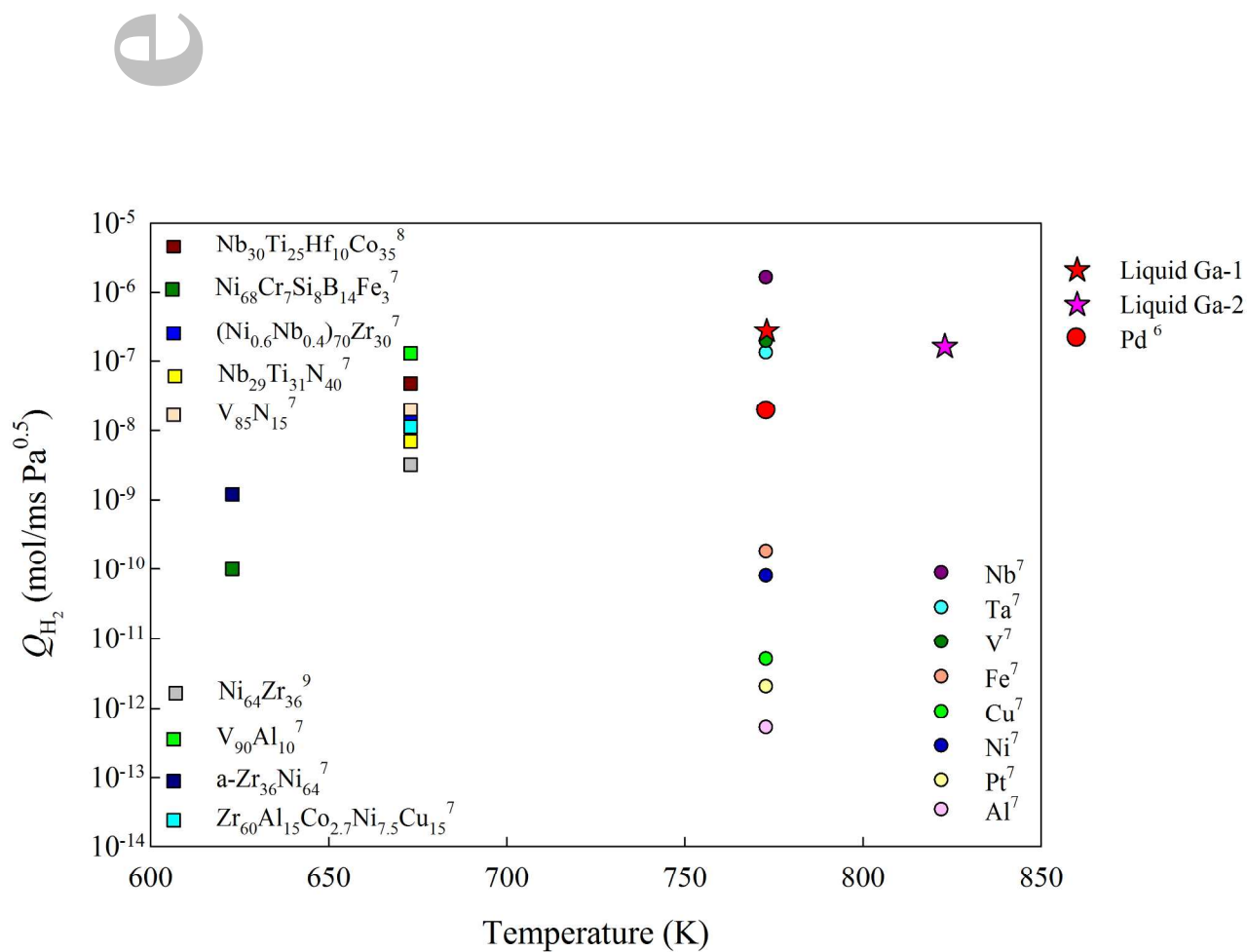


Figure 1. Hydrogen permeability of dense liquid gallium membrane, metals and amorphous metals between 623~823 K.<sup>6-9</sup>

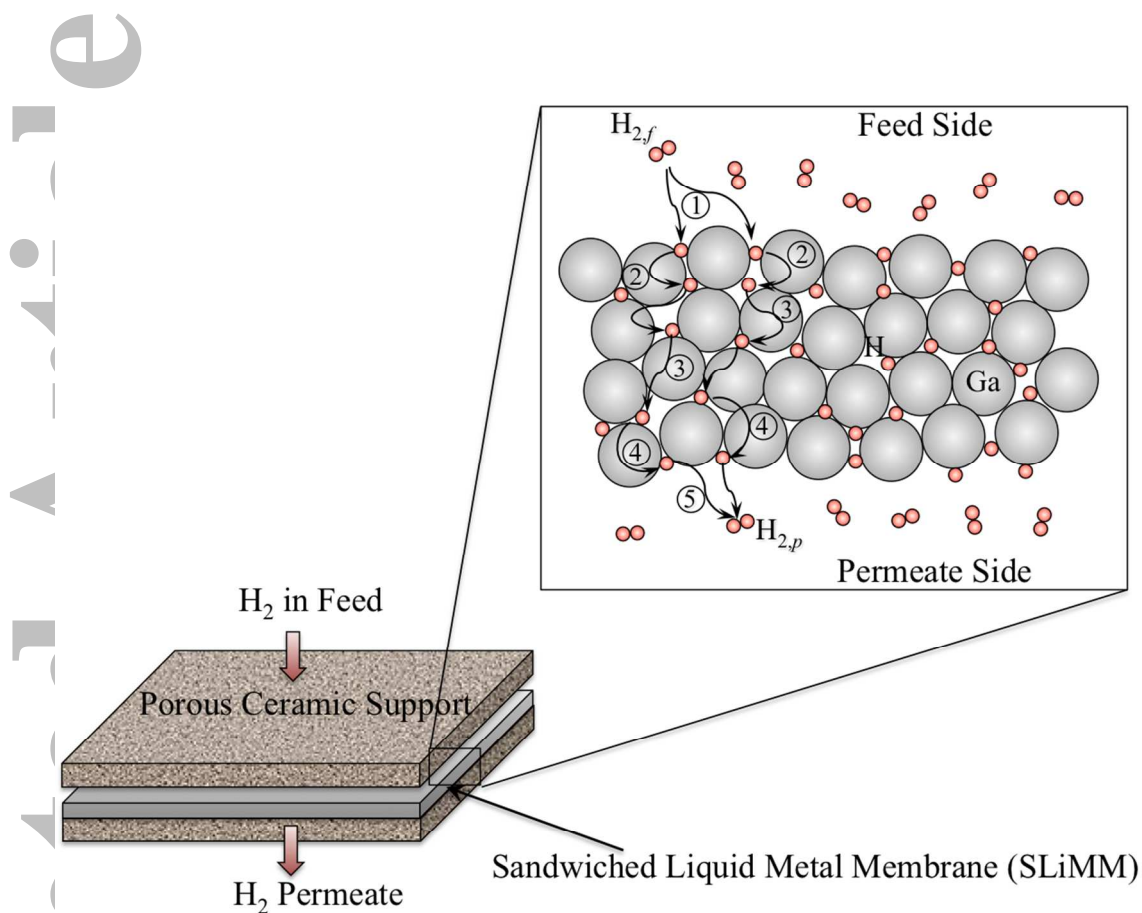


Figure 2. A schematic of the H<sub>2</sub> permeation process through a dense liquid metal membrane involving sequential steps of: ① surface dissociative adsorption, ② subsurface penetration, ③ bulk metal diffusion, ④ egression to surface, and ⑤ reassociation of H atoms on the surface to form molecular H<sub>2</sub>.

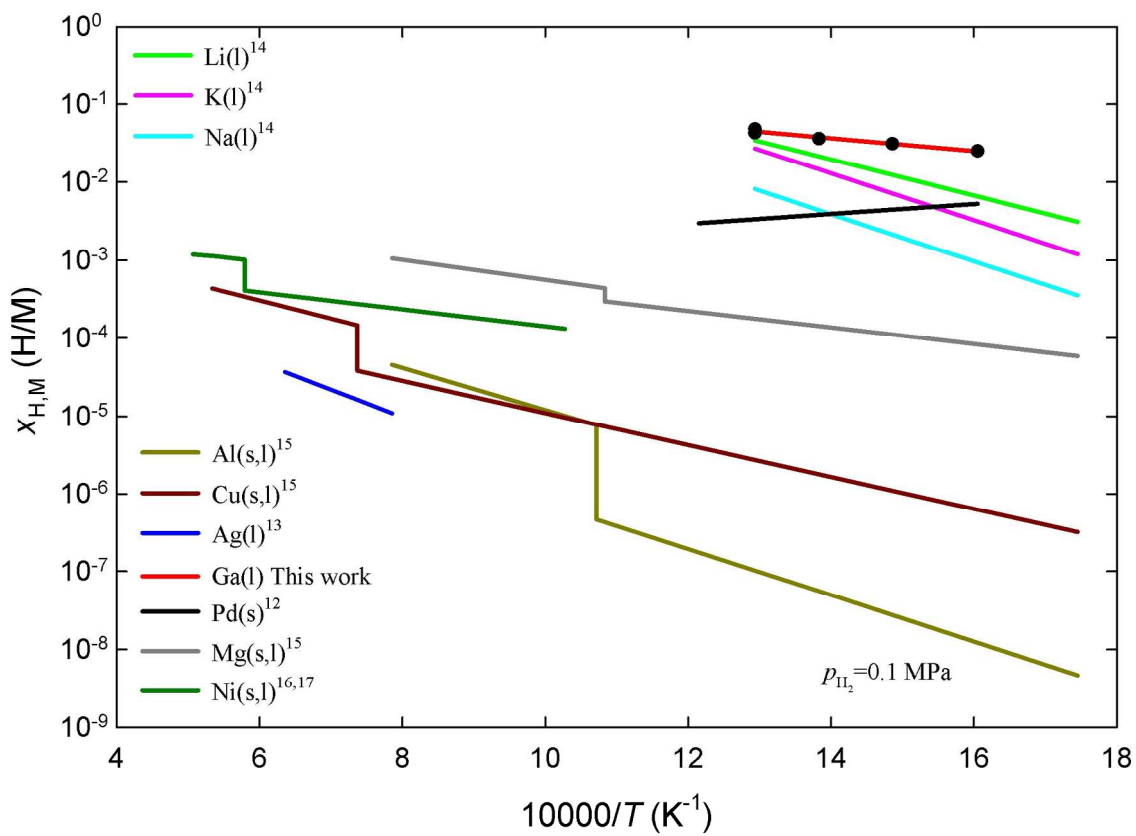


Figure 3. Solubility of hydrogen in various liquid and solid metals versus inverse absolute temperature for hydrogen pressure  $p_{H_2} = 0.1$  MPa.<sup>12, 14-17</sup>

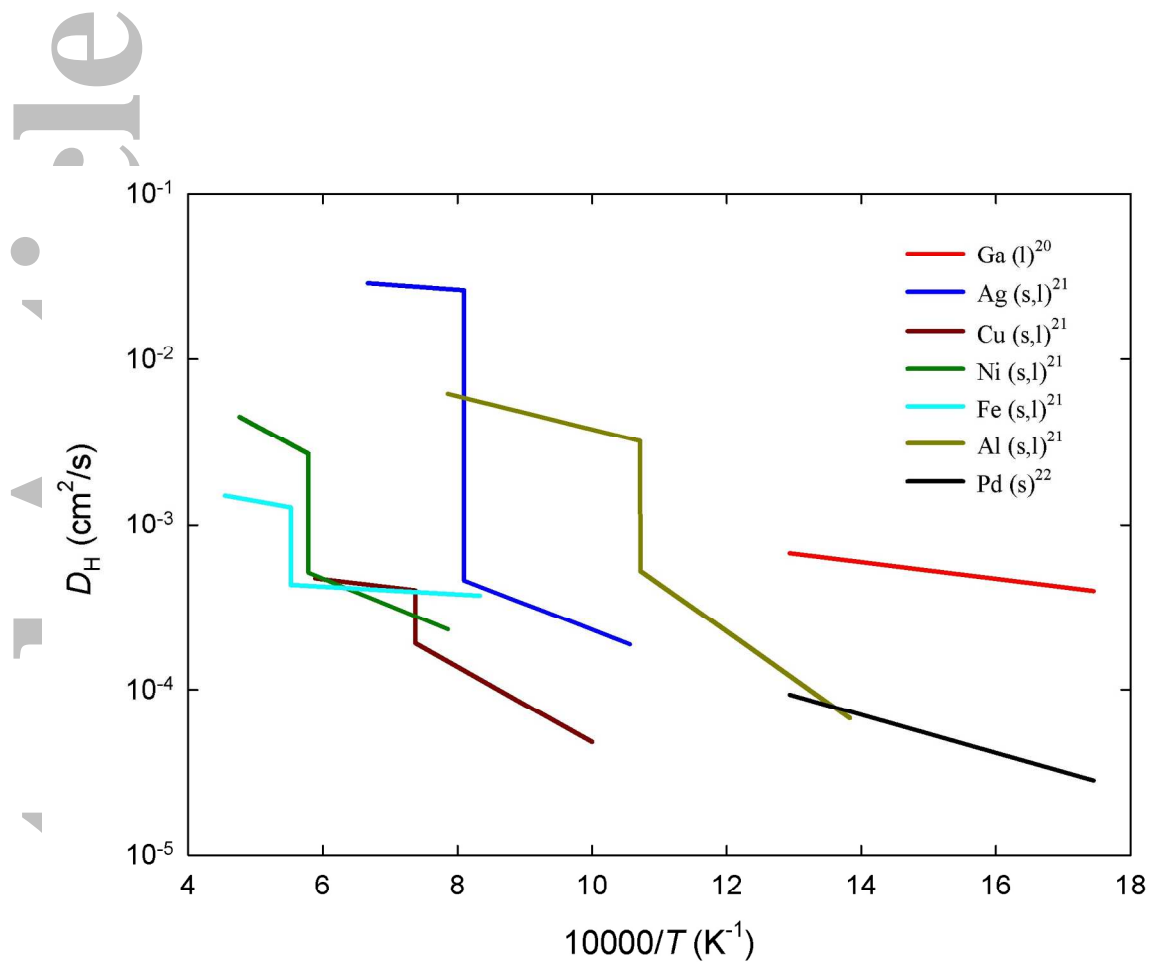


Figure 4. Hydrogen diffusion coefficient in some metals in their liquid and solid states as a function of inverse absolute temperature.<sup>20-22</sup>

icle

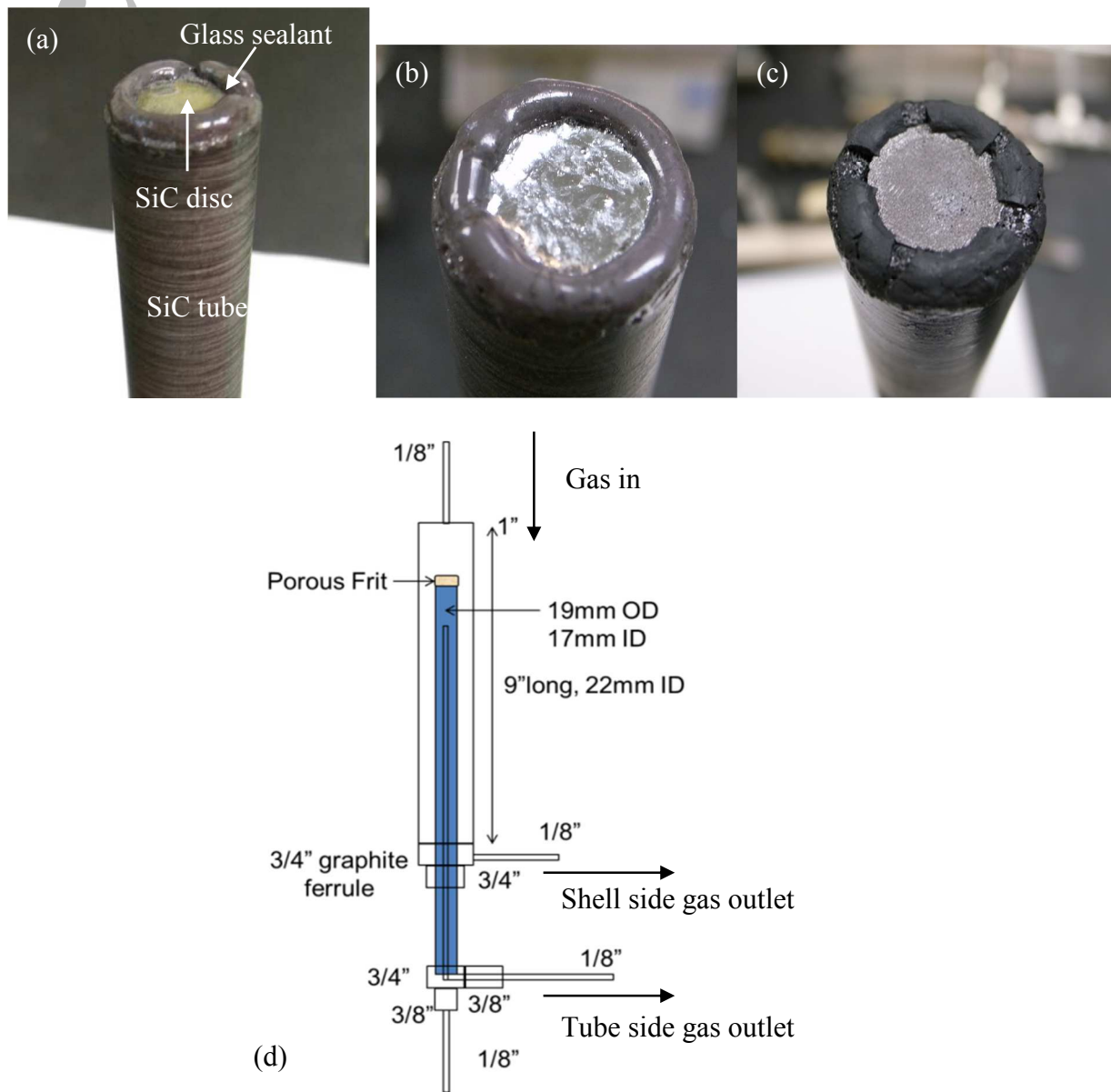


Figure 5. (a) SiC porous disc attached to nonporous SiC tube with glass paste seal, (b) with deposited gallium film, (c) sandwiched liquid metal membrane and (d) scheme of hydrogen permeation setup.

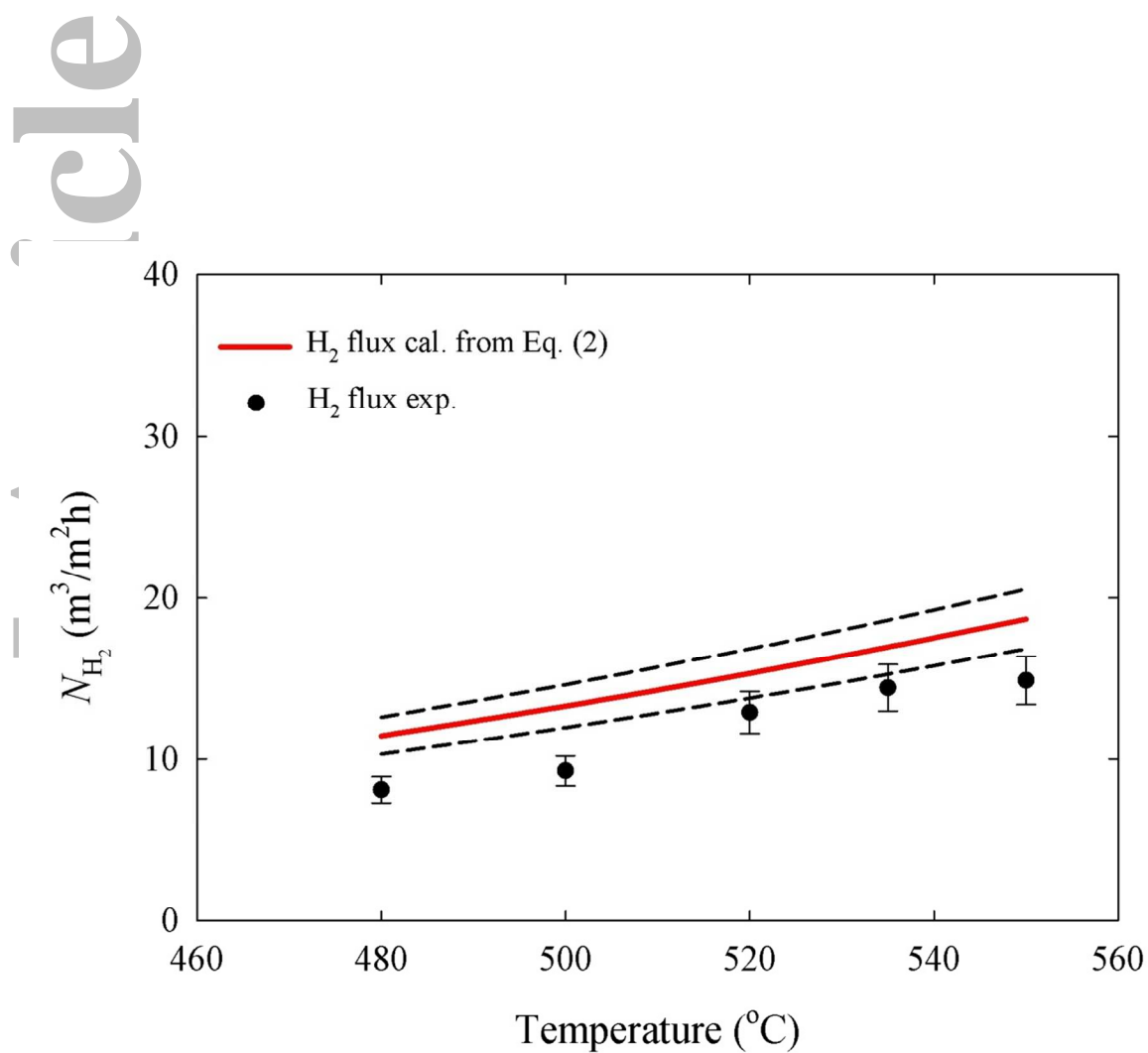


Figure 6. Measured versus calculated hydrogen flux based on independently measured solubility and diffusivity in liquid gallium membrane.

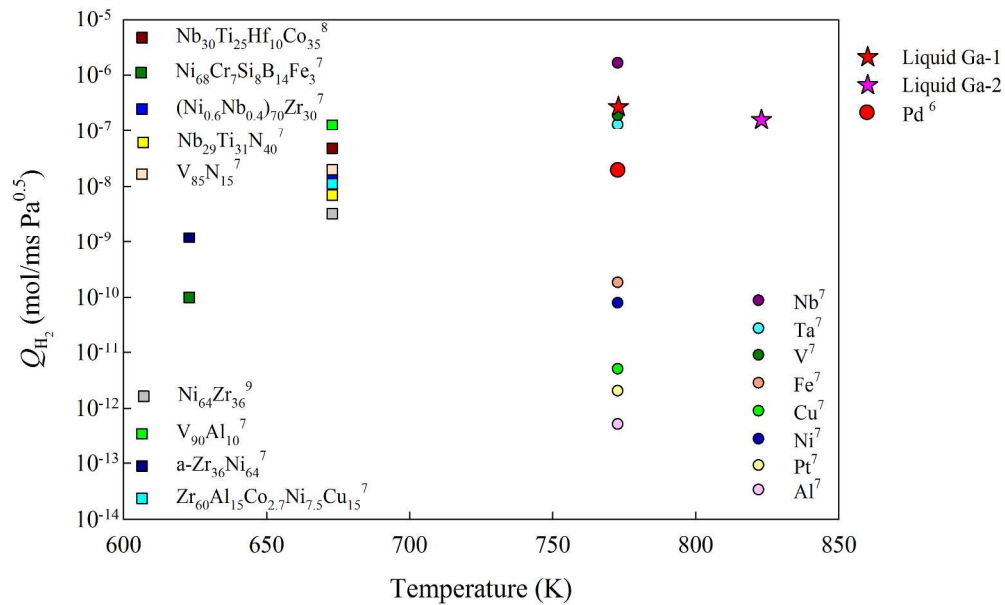


Figure 1. Hydrogen permeability of dense liquid gallium membrane, metals and amorphous metals between 623~823 K.<sup>6-9</sup>

254x190mm (300 x 300 DPI)

Accep

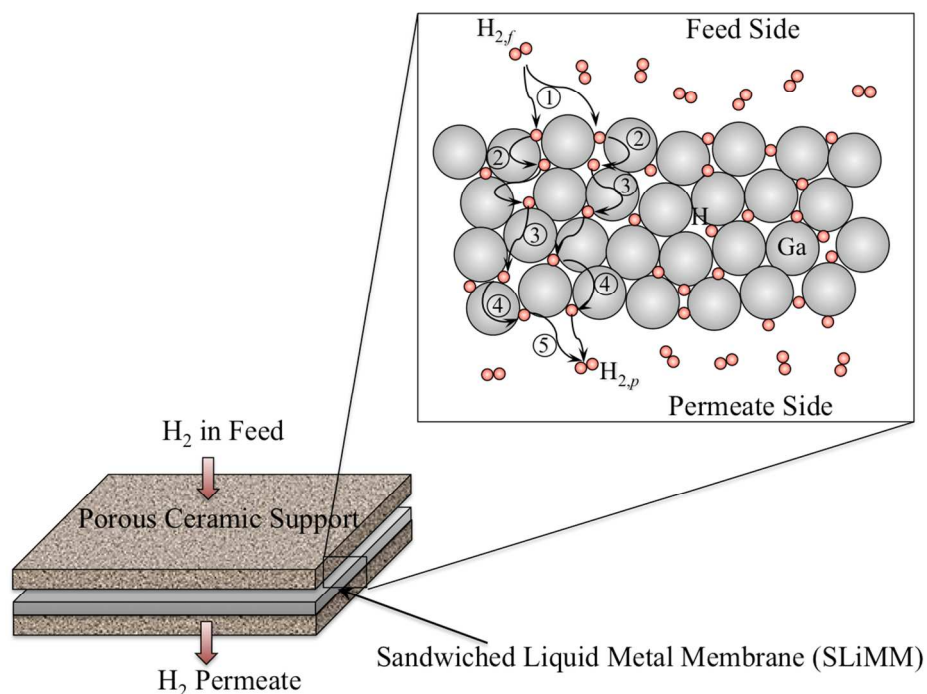


Figure 2. A schematic of the  $H_2$  permeation process through a dense liquid metal membrane involving sequential steps of: 1 surface dissociative adsorption, 2 subsurface penetration, 3 bulk metal diffusion, 4 egression to surface, and 5 reassociation of H atoms on the surface to form molecular  $H_2$ .

221x155mm (300 x 300 DPI)

Accep

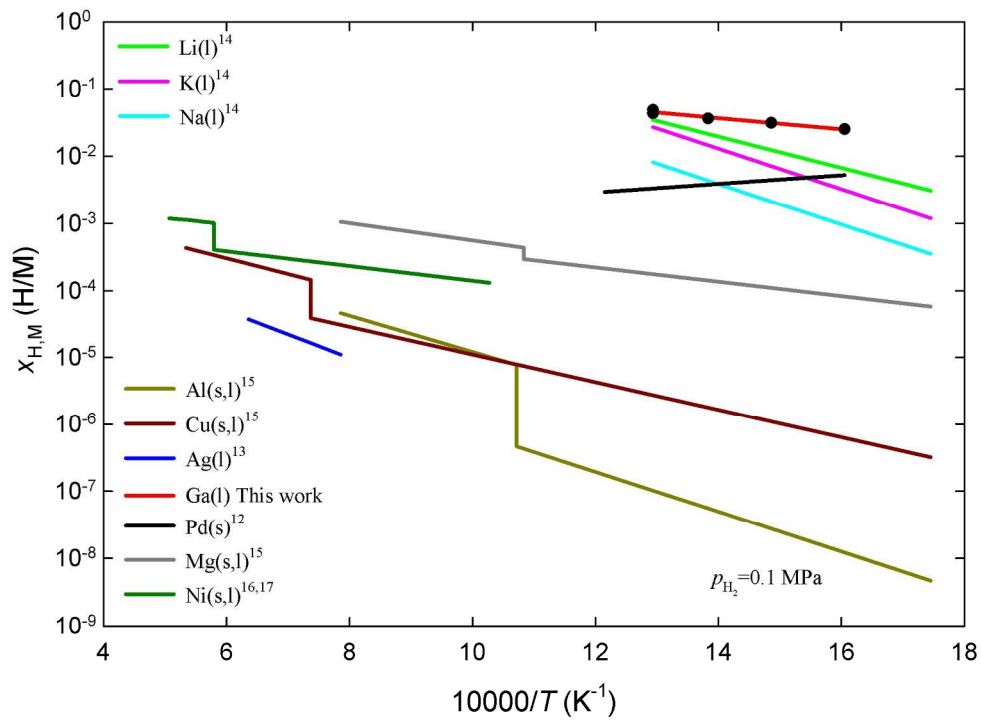


Figure 3. Solubility of hydrogen in various liquid and solid metals versus inverse absolute temperature for hydrogen pressure  $p_{H_2}$  MPa.<sup>12, 14-17</sup>

197x146mm (300 x 300 DPI)

Accep

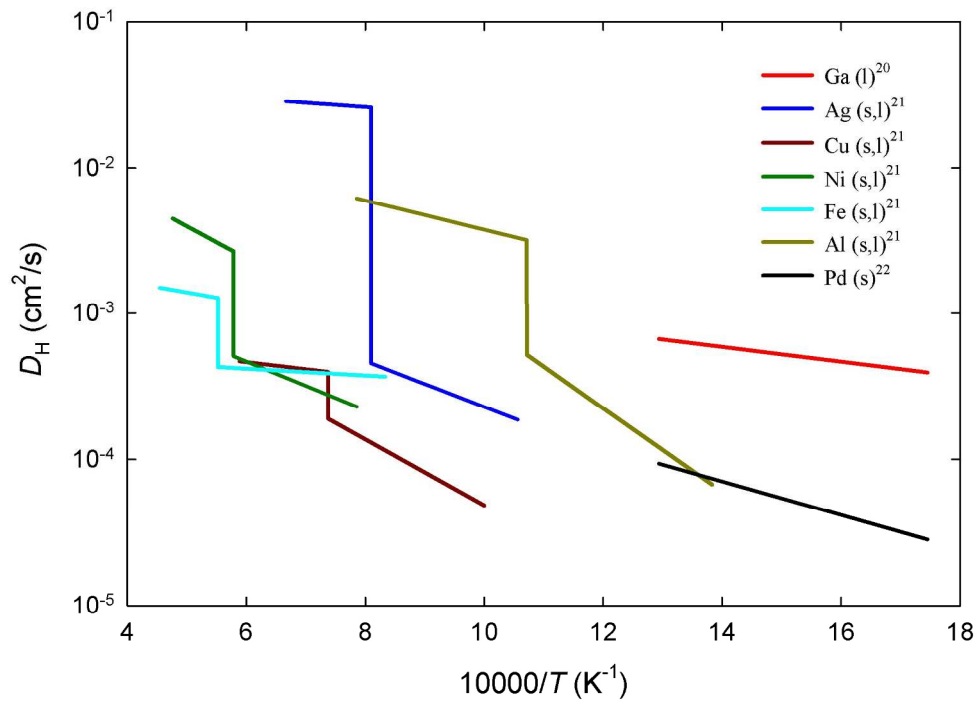


Figure 4. Hydrogen diffusion coefficient in some metals in their liquid and solid states as a function of inverse absolute temperature.<sup>20-22</sup>

193x138mm (300 x 300 DPI)

Accep

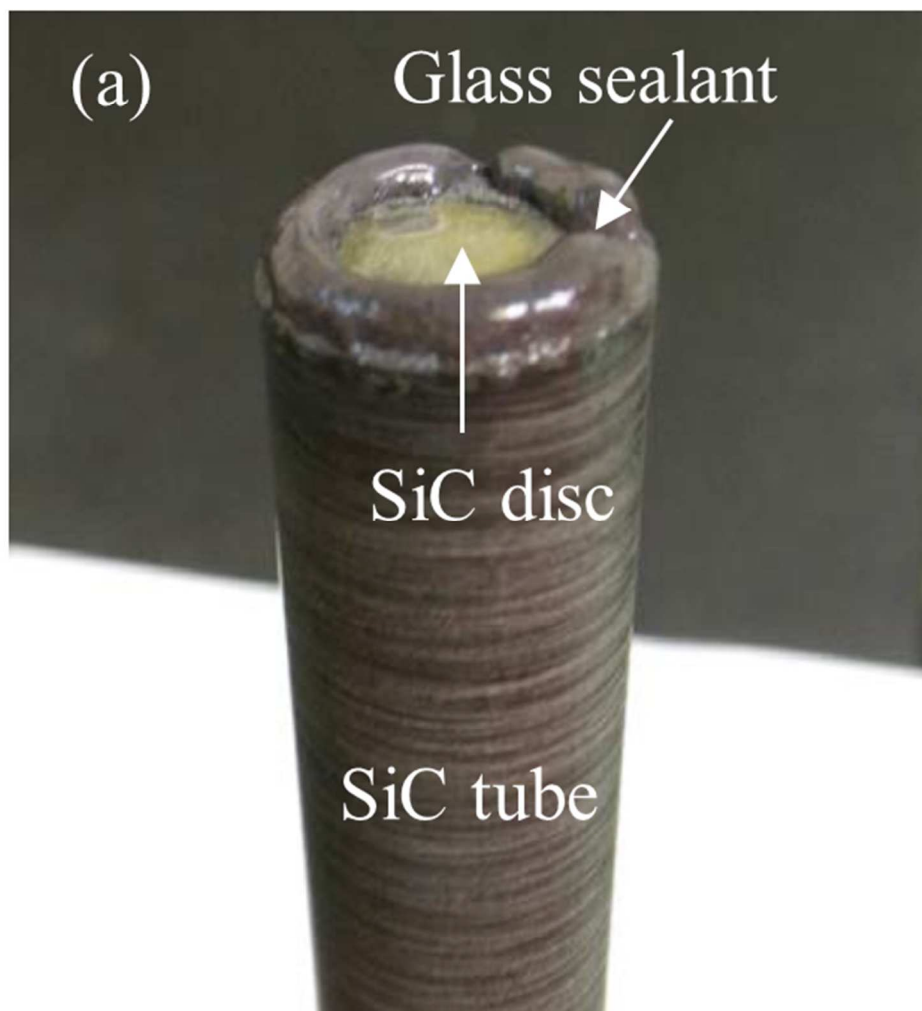
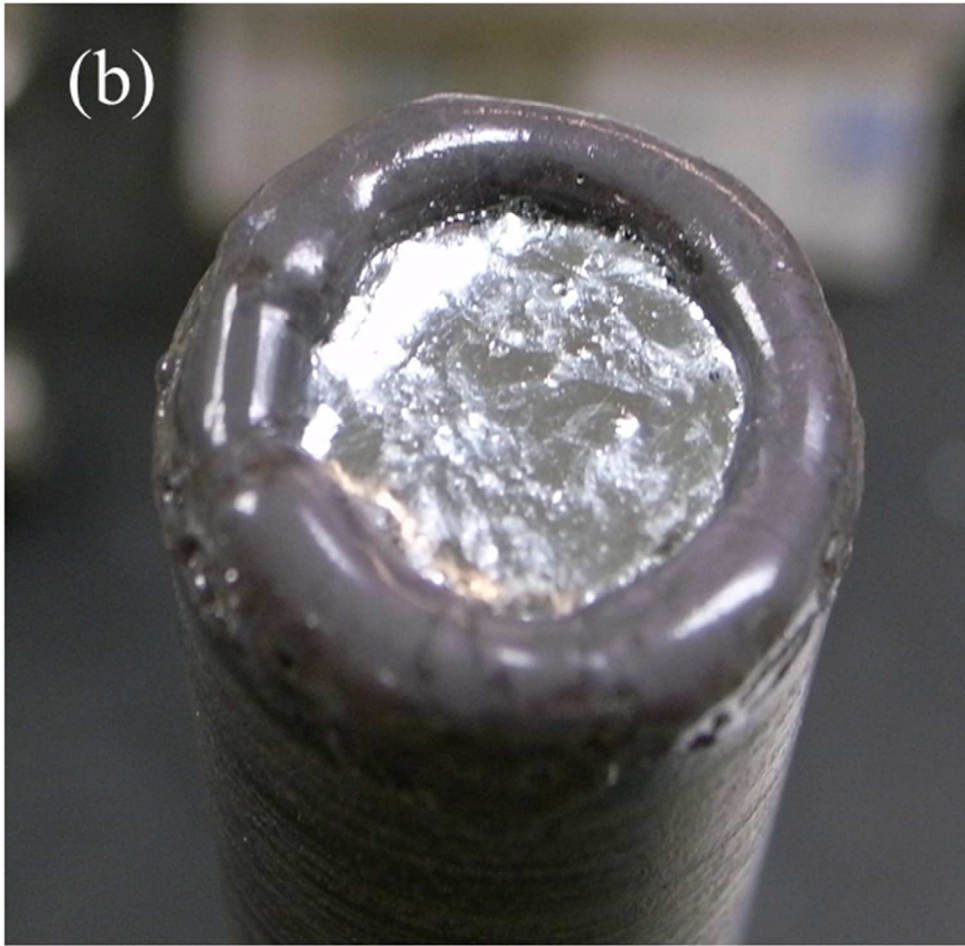


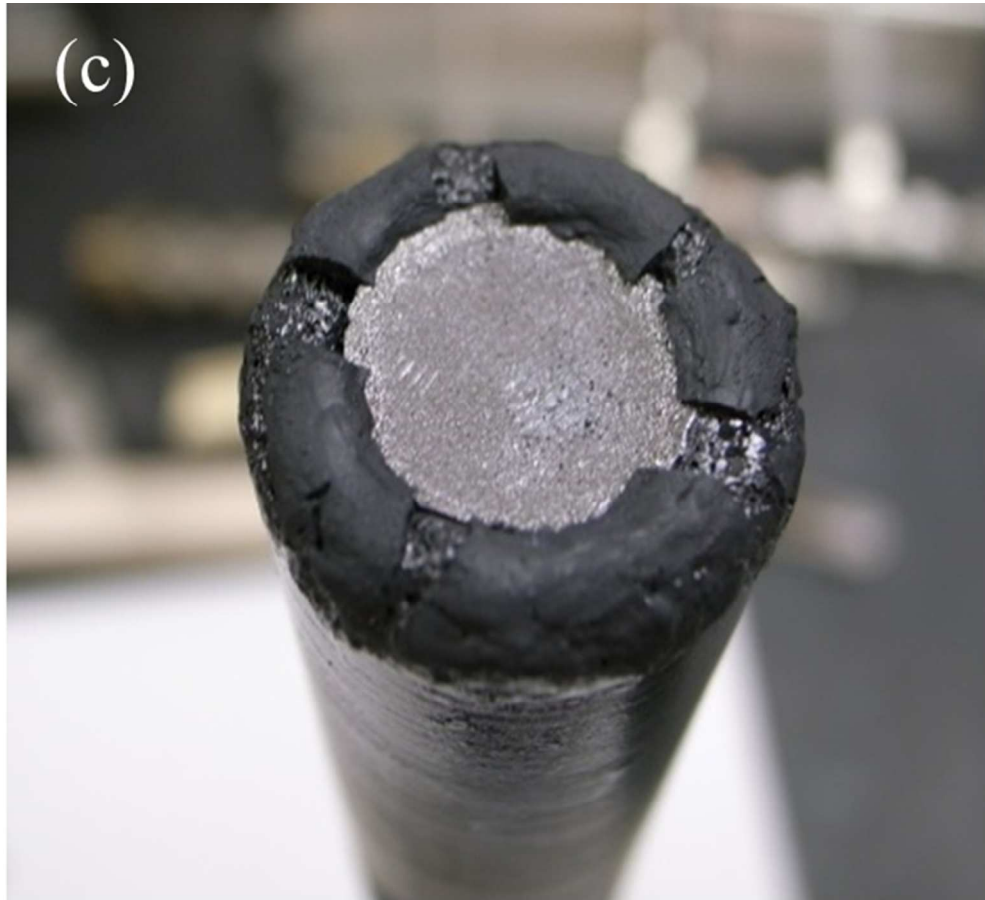
Figure 5. (a) SiC porous disc attached to nonporous SiC tube with glass paste seal, 56x59mm (300 x 300 DPI)

AC



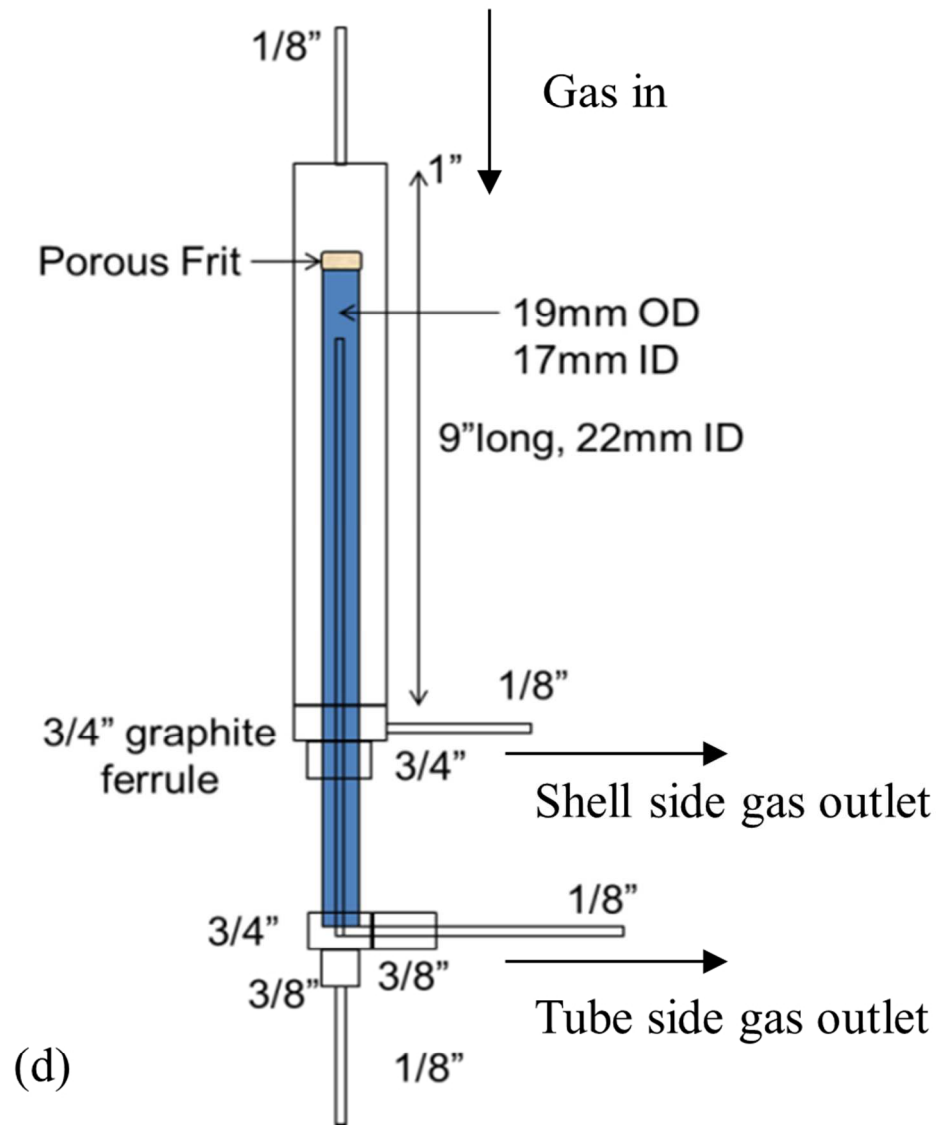
(b) with deposited gallium film,  
54x52mm (300 x 300 DPI)

Acc



(c) sandwiched liquid metal membrane and  
56x50mm (300 x 300 DPI)

Acc



(d) scheme of hydrogen permeation setup.

86x99mm (300 x 300 DPI)

A.

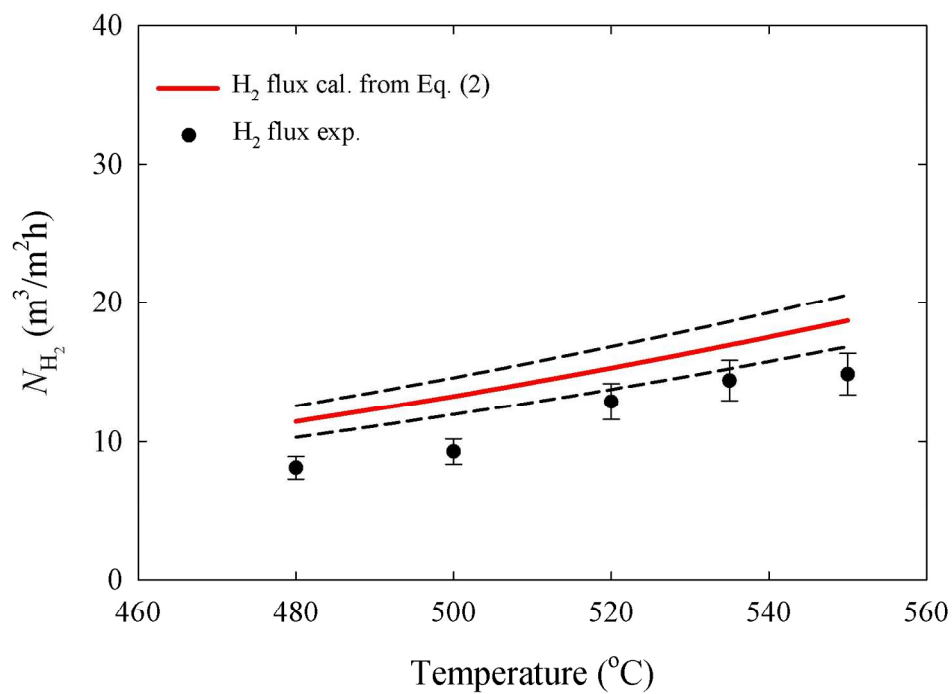


Figure 6. Measured versus calculated hydrogen flux based on independently measured solubility and diffusivity in liquid gallium membrane.

160x114mm (300 x 300 DPI)

Accep.